Report of the internship

Study of optical and radiative properties of cirrus clouds from ground based measurements using the synergy between Lidar and Multi-channel infrared radiometry

Presented by

WU Junteng

Environment Atmosphere 2014-2015

LOA UMR/CNRS 8518

Supervisors: Gérard BROGNIEZ and Frédéric PAROL

Abstract

On account of their large spatial and temporal extension and their low temperature due to the high altitude, cirrus clouds have a major influence on the earth energy balance through their effects on the incoming solar and the outgoing infrared radiations. Moreover, It's well known that the climatic impact of cirrus clouds is well recognized but not exactly determined because their optical properties are still not known very well. Then, the radiative impact of the cirrus cloud depends on its temperature, its altitude, its optical thickness, and, significantly, its micro-physical properties (Liou, 1986). Indeed, it is composed of ice crystals with extremely large variability in shape and size whose optical properties modeling is very difficult.

Basically, this report presents a method to establish the optical properties from ground-based measurements, using the synergy between active (Lidar) and passive (multi-channel infrared radiometry) remote sensing. It's helpful for the research of the urban climatic impact, especially to the influence by the cirrus-like, the production of the human behavior.

Keywords: optical properties, cirrus clouds, Lidar, IR radiometry, climatic signification

Table of Contents

Introduction

Cirrus clouds which continuously cover more than 20% of the Earth's surface are located at a high altitude of around 10 km, depending of the altitude and the season. It is important to study these types of clouds because of its great influence on the radiation balance of the planet.

Long time ago, many people started to learn how could the climate be changed by the clouds. Whereas, cirrus, as a kind of high cloud, draws attentions for the last two centuries due to its concealment. Surprisingly, neither rain, nor snow, it always appears in the clear sky in the form of fine thread. However, to our delight many mysteries of the cirrus are gradually discovered so far. During this internship, my study focused on the optical properties of the local cirrus (January to March 2015) which is situated in M'Bour (Senegal) by using the Lidar and the multi-channel infrared radiometry.

In this part, I will introduce the short history of the cirrus cloud research generally, the official definition of different types of cirrus, background and the purposes.

1. History

Cirrus cloud is formed only by ice crystals, without the liquid droplets. This important character is not easy to provide many centuries ago. The low clouds can bring precipitations, it is obvious the first idea in the head. However, the cirrus product nether rain, nor snow.

Perhaps Anaxagoras de Clazomenae (500-428 BC) was the first person who has the idea about the formation of the cirrus clouds. He believes that hot air rises and it will descent with the formation of ice particles (Lynch et al, 2001). During the two thousand years, there is no progress on the cirrus clouds study. Until the year 1673, Descartes found that the halo phenomenon is different from the rainbow sky because the halo may appear in the clear sky (Lynch et al, 2001). This year, he published the Discourse on Method by three parts:

Dioptrics, Metrology and Geometry. And then, he surmised that the halo phenomenon (22°) is caused by ice crystals.

In 1803, when Luke Howard published an article on classic clouds, he used the word "cirrus" which comes from Latin. He was the first person to use "cirrus" to express morphology of the clouds. Later, the scholar completed the cloud system. Until 1957, the cirrus has begun to be observed by using satellites and Lidar. After some years, Dowling and Radke (1990) proposed the cirrus properties summarized in Table 1.

Table 1 Properties of cirrus cloud

Properties	Average	Range
Thickness	1.5 km	0.1-8 km
Altitude	9 km	4-20 km
Concentration	30/L	10^{-4}-10^{4}/L
Density of ice	0.025 g/m^3	10^{-4}-1.2 g/m^3
Radius	250 µm	1-8000 µm
Adapted from Dowling and Radke (1990)		

2. Official definition of different types of cirrus

Different types of cirrus can be present in the atmosphere. The official definition of the different types of cirrus is given by the World Meteorological Organization (WMO):

Cirrus*: clouds separated in the form of white, delicate filaments or patches or narrow bands, white or mostly white. These clouds have a fibrous (hair) or a silky sheen, or both.*

Cirrocumulus*: patch, sheet or thin white cloud without shading, composed of very small elements in the form of grains, ripples, etc., merged or separate, and more or less regularly arranged; Most elements have an apparent width of less than one degree.*

Cirrostratus*: Sailing transparent and whitish cloudy, with fibrous (hair) or smooth, fully or partially covering the sky, and generally resulting in halo phenomena.*

International Meteorological Vocabulary WMO - No. 182

3. Background of the cirrus research

It is well known that the impact of cirrus clouds on Earth's energy budget is poorly quantified as they affect the radiation budget in two antagonistic effects (Liou, 1986). On the one hand, they reflect part of the incident solar radiation to space; on the other hand, they participate in the greenhouse effect because they trap infrared radiation emitted by the lower layers of the atmosphere. Generally, the first effect tends to cool the atmosphere, while the second one tends to warm it.

We found that the importance of these two effects depends on their thickness: when the cloud is thin and its albedo is low, the greenhouse effect warm the atmosphere; when the cloud is thick and its high albedo has the effect of cooling the atmosphere. That influence is still poorly quantified because these clouds are made of ice crystals with different dimensions and shapes, making it difficult to model their optical properties.

The first method to study the cirrus consists to use in-situ measurements by aircraft. It is important to mention that, due to their altitude, these clouds are difficult to access. And their study by remote sensing (from ground based or satellite measurements) appears. To be delighted that such studies have already been conducted in the laboratory, on both ground measurements (Flamant et al, 1989; Ansmann et al, 1993) and satellite measurements based on the work of (Inoue 1985; 1987), (Parol et al, 1991), (Brogniez et al, 1995), (Dubuisson et al, 2008).

4. Purposes of the internship

Compared with the remote sensing by satellite, the use of ground-based instrument is an another method for study the local cirrus. During this internship, I used the data from the Lidar and Infrared radiometer which are installed in M’Bour (Senegal), performing measurements routinely, to analysis the properties of the cirrus. After finding some periods with cirrus, my goal consisted to calculate the cirrus effective emissivity, crystal dimension and the Ice Water Path (IWP). Furthermore, I also did some statistic analysis to find the characteristics of the cirrus cloud in M’Bour.

During the internship, prospectively, the language FORTRAN 77 was applied to write programs of calculations.

Instruments

As has been noted, the Lidar visible light is a suitable tool to study cirrus clouds. It could provide a characterization of some properties (altitude, geometrical thickness, optical thickness). In particular, the synergy between the multi-channel infrared radiometry measurements from cirrus and Lidar measurements, provide the emissivity, the mean dimension and concentration of ice crystal. Moreover, It is also helpful to better construct the radiative transfer models and improve our knowledge of cirrus successfully.

1. Lidar at 532nm

As we all know, remote sensing by laser or LIDAR, an acronym of the expression "light detection and ranging", is a remote sensing technology based on the analysis of the properties of a beam back scattered. This kind of observation is called active remote sensing.

Currently, Lidar works by using a discontinuous and periodical laser. With different particle individual, the power back is not the same. Expression of the vertical distribution of back scattered Lidar is given by the following equation (Russell et al, 1979) :

$$P(\mathrm{z}) = \frac{K}{z^2}\beta(z)\exp\left[-2\int_0^z \alpha(z')dz'\right] \tag{2-1}$$

where K is the instrumental constant in $\mathrm{Js^{-1}m^2}$; $\alpha(z)$ is the total extinction coefficient in $\mathrm{m^{-1}}$ (absorption+attenuation) at the altitude z; $\beta(z)$ presents the back scattered coefficient at the altitude z expressed in $\mathrm{m^{-1}sr^{-1}}$.

To visually display the data, the following photographer is used. In Figure (2-1), the color presents the value of the $Ln(P(z)\cdot z^2)$ which is respected by the equation (2-1). The red color part corresponds to high value of the back scattered Lidar signal. In another word, blue color parts corresponds to the weaker signal.

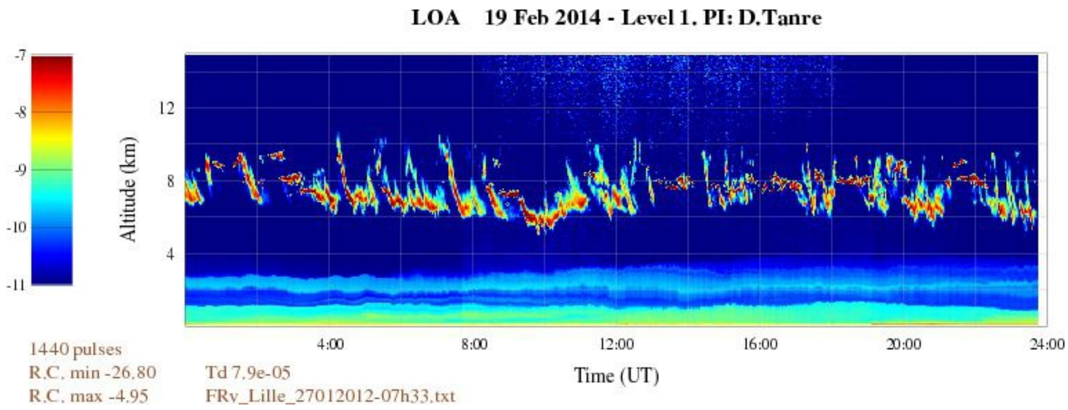

Figure (2-1)

This figure shows the back scattered signal as a function of time and altitude. The aerosol layer is situated in the base and the cirrus layer is situated at an altitude of around 8 km.

2. Multi-channel infrared radiometry

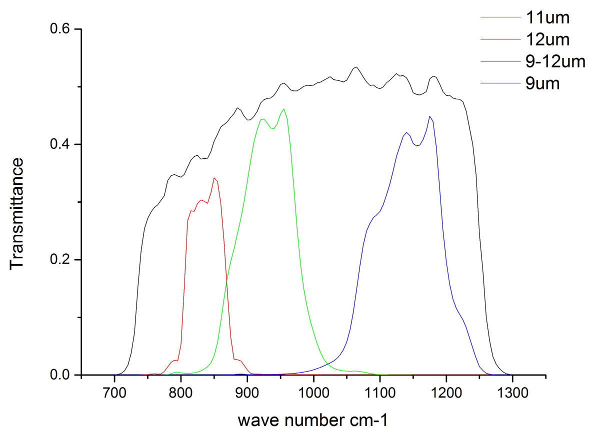

Figure (2-2)

The three colors present the transmission between the nature luminance and the luminance measured in the function of wave number.

Thermal Infrared radiometer (TIR) is an instrument which receives the infrared emission from a given source. This is a kind of passive remote sensing because the source is not from the instrument. In the meantime, I used the data from the Multi-channel thermal infrared radiometry (CLIMAT CE-312). As shown in the Figure (2-2), it is equipped with 3 different channels: centered at 8.7 µm, 10.5 µm and 12 µm which are named C09, C11 and C12 respectively. (Legrand et al, 2000; Brogniez et al, 2003).

Methodology

1. Hypothesis

In our case of the study, the instruments are installed at ground level at an altitude about 0 km. With the movement of the clouds, they will measure many different pieces of clouds. At the same time, we consider that the altitude and the thickness of cirrus be constant. Accordingly, we found that it helps to study the cirrus simply and it supposes a standard to compare with others.

We have restricted this work to a feasibility study. In the first approximation, in order to simplify the problem, we have not taken into account the light scattering process in the atmosphere within the thermal infrared range. This approximation permits to solve the problem with simple analytic equations.

In particular, Rayleigh scattering by molecules (in λ^{-4}) is weak, as well as the scattering by little aerosols (in $\lambda^{-\alpha}$ with α=2). The light scattering in the cirrus is also weak. One reason is that we consider ice crystals as purely absorbable particles; another important reason is that the distribution of the source of radiation is obviously much more isotropic than in the shortwave, thus, reducing the role of scattering.

Of course, a deeper study will required to take into account the light scattering.

2. The spatial orientation of the cirrus clouds

With the help of Lidar backscattered signal, we can clearly know the altitude of the obstacle in the atmosphere.

For example, the Figure (3-1) shows us the signal on 2015/03/17 in M'Bour. This figure shows that the cirrus cloud is at the altitude of around 12 km. To get the precise result, we need a signal without clouds to obtain a reference (Flamant et al, 2008).

A) The trace of the theoretical signal only by molecule

In the equation (2-1), we can observe that to get the constant of the instrument, 3 parameters must to be estimated at each altitude z: the power $P(z)$ of the back scattered signal, the extinction coefficient $\alpha(z)$ and the back scattered coefficient $\beta(z)$. We have $\beta(z)=\frac{p(z)\sigma(z)}{kT(z)}$, where $p(z)$ and $T(z)$ are the atmosphere pressure and the temperature; $\sigma(z)$ is the scattering coefficient which is estimated for the instrument, wavelength i.e. 532nm; The extinction coefficient is given by $\alpha(z)=\frac{8\pi\beta}{3}$ (Flamant et al, 2008).

Above all, we can calculate the average of the instrument constant K by using the signal between 4-6 km in the clear situation. Using the obtained value of K, we can get the theoretical value of $Ln(P(z)\cdot z^2)$ as function of altitude which is presented as the red line in the Figure (3-1).

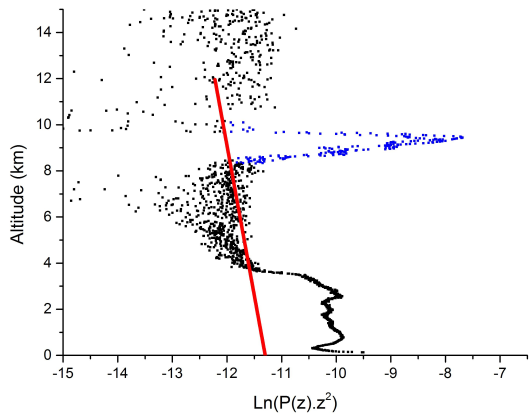

Figure (3-1)
The blue points present the mainly location of the cirrus clouds in the atmosphere; the red line presents the theoretical signal in the situation of clear.

B) Geometrical properties of the cirrus cloud

To compare with the theoretical signal trace, it's easily to get z_b and z_t which are the altitude of the base and the top of the cloud. For the cirrus cloud mean altitude, we use the weighted average of the altitude, where the difference of the signal between theory and measurement is the weight.

Hence, we can get the precise geometrical properties of the cirrus cloud

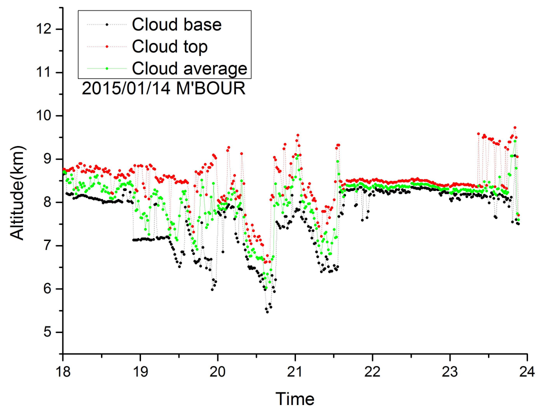

Figure (3-2)
The red points present the top of the cloud; the green points present the weighted average of the cloud; the black points present the base of the cloud.

on 2015/01/14 between 18:00 and 24:00 UT in M'Bour, which is presented in the Figure (3-2). We can see that the period between 21:30-23:30 is perfect to study the cirrus cloud.

3. Emissivity of the cirrus clouds

A) Infrared radiation on the ground from the clear sky

We supposed a plane-parallel atmosphere, and the scattering is neglected. The radiative transfer at the wavelength λ for a thin layer of atmosphere dz located at the altitude z is written with this differential equation:

$$\frac{dI_{\lambda}(z)}{dz} = -k_{\lambda}\left\{I_{\lambda}(z) - B_{\lambda}[T(z)]\right\} \tag{3-1}$$

where $B_{\lambda}[T(z)]$ is the Planck function at temperature $T(z)$; k_{λ} is the absorption coefficient of the atmosphere layer and $I_{\lambda}(z)$ is the radiance at the altitude z.

Separating the upward and downward radiance, we finally obtain, after integration of the differential equation (3-1), the downward zenithal radiance at the level z_o:

$$I_{\lambda}^{\downarrow Clear}(z_o) = -\int_{z_0}^{\infty} B_{\lambda}[T(z)] \frac{\partial t_{\lambda}(z_o, z)}{\partial z} dz \tag{3-2}$$

where $t_{\lambda}(z_o, z)$ is the transmission of the atmosphere between z_0 and z for the wavelength λ.

B) Infrared radiation to the ground from the cloudy sky

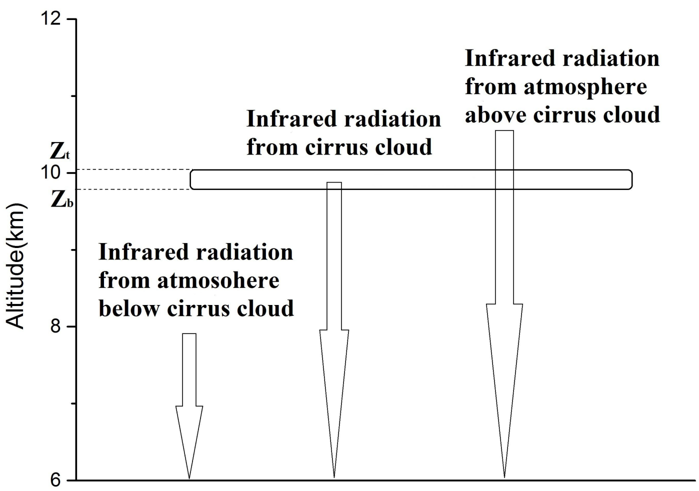

Figure (3-3)
The model from the hypothesis, the radiation to the ground is from 3 parts.

In the case of the sky covered by cirrus cloud, as shown in the Figure (3-3), we separate the equation (3-2) into 3 parts:

- the part below the cirrus (between the altitude z_o and z_b)
- the part above the cirrus (between the altitude z_t and ∞)
- the part inside the cirrus (between the altitude z_b and z_t)

We obtain the radiance at ground under a cirrus cloud:

$$I_\lambda^{\downarrow Cirrus}(z_o) = -\int_{z_o}^{z_b} B_\lambda[T(z)]\frac{\partial t_\lambda^{Clear}(z_o,z)}{\partial z}dz - \int_{z_o}^{z_t} B_\lambda[T(z)]\frac{\partial t_\lambda^{Cirrus}(z_o,z)}{\partial z}dz - \int_{z_t}^{\infty} B_\lambda[T(z)]\frac{\partial t_\lambda^{Clear}(z_o,z)}{\partial z}dz \quad (3\text{-}3)$$

where $t_\lambda^{\mathrm{Cirrus}}(z_o,z)$ is the transmission of the atmosphere with cirrus between z_b and z for the wavelength λ, and $t_\lambda^{\mathrm{Clear}}(z_o,z)$ is the transmission of the clear atmosphere between z_o and z.

C) Infrared radiation from the cirrus cloud

In order to extract the proper influence of the cirrus on the measurements, we express the difference between cloud and clear situations. And then we obtain a relation where only the temperature of the cloud remain:

$$\left[I_\lambda^{\downarrow Cirrus} - I_\lambda^{\downarrow Clear}\right](z_o) = -\int_{z_b}^{z_t} B_\lambda[T(z)]\frac{\partial\, t_\lambda^{Cirrus}(z_o,z)}{\partial z}dz - \int_{z_b}^{z_t} B_\lambda[T(z)]\frac{\partial\, t_\lambda^{Clear}(z_o,z)}{\partial z}dz \quad (3\text{-}4)$$

With the hypothesis of temperature between z_b and z_t is constant, the Plank's function $B_\lambda[T(z)]$ is also constant in this interval. Let T_{Cirrus} and T_{Clear} be the temperature of the clear and cloudy sky between z_b and z_t, which will be used from Wyoming University raido sounding, we obtain:

$$\left(I_\lambda^{\downarrow Cirrus} - I_\lambda^{\downarrow Clear}\right)(z_o) = -B_\lambda(T_{Cirrus})\left[t_\lambda^{Cirrus}(z_o,z_t) - t_\lambda^{Clear}(z_o,z_b)\right] - B_\lambda(T_{Clear})\left[t_\lambda^{Clear}(z_o,z_t) - t_\lambda^{Clear}(z_o,z_b)\right] \quad (3\text{-}5)$$

We will use two remarks:

I. $t_\lambda^{Cirrus}(z_o,z_t) = t_\lambda^{Clear}(z_o,z_b)\times t_\lambda^{Cirrus}(z_b,z_t)$

II. Around the altitude of 10 km, $t_\lambda^{\mathrm{Clear}}(z_o,z)$ is low and varies little on the thickness of the cloud, which enables writing as: $t_\lambda^{Clear}(z_o,z_t) \approx t_\lambda^{Clear}(z_o,z_b)$

Considering these two comments, we obtain:

$$\left(I_\lambda^{\downarrow Cirrus} - I_\lambda^{\downarrow Clear}\right)(z_o) = \left[1 - t_\lambda^{Cirrus}(z_b,z_t)\right] B_\lambda(T_{Cirrus})\, t_\lambda^{Clear}(z_o,z_b) \quad (3\text{-}6)$$

Assume that the scattering in the cloud is neglected, the effective emissivity of the cloud will be written as:

$$\varepsilon_{\lambda}^{Cirrus} = \left[1 - t_{\lambda}^{Cirrus}\left(z_b, z_t\right)\right] \tag{3-7}$$

Finally we get:

$$\left(I_{\lambda}^{\downarrow Cirrus} - I_{\lambda}^{\downarrow Clear}\right)\left(z_o\right) = \varepsilon_{\lambda}^{Cirrus}\ B_{\lambda}\left(T_{Cirrus}\right) t_{\lambda}^{Clear}\left(z_o, z_b\right) \tag{3-8}$$

D) Measurements in a small spectral range *Δλ*

As mentioned in the Figure (2-2), the infrared radiometer measure the radiation in the spectral interval *Δλ*, which is about 1 μm FWHM. The normalized integrated radiation in this spectral interval is written as:

$$L_{\Delta\lambda}^{\downarrow} = \frac{\int_{\Delta\lambda} I_{\lambda}^{\downarrow} f(\lambda) d\lambda}{\int_{\Delta\lambda} f(\lambda) d\lambda} \tag{2-9}$$

Where $f(\lambda)$ is the transmission as a function of λ.

Then this gives:

$$\left(L_{\Delta\lambda}^{\downarrow Cirrus} - L_{\Delta\lambda}^{\downarrow Clear}\right)\left(z_o\right) = \frac{\int_{\Delta\lambda} \varepsilon_{\lambda}^{Cirrus}\ B_{\lambda}\left(T_{Cirrus}\right) t_{\lambda}^{Clear}\left(z_o, z_b\right) f(\lambda) d\lambda}{\int_{\Delta\lambda} f(\lambda) d\lambda} \tag{3-10}$$

With the wavelength, the variation of $t_{\lambda}^{\mathrm{Clear}}\left(z_{\mathrm{o}}, z\right)$ is faster than $B_{\lambda}\left[T_{Cirrus}\right]$ and $\varepsilon_{\lambda}^{Cirrus}$. Then, if we call $\bar{\varepsilon}_{\Delta\lambda}$ and $L_{\Delta\lambda}(T_{Cirrus})$ as the effective emissivity and the mean Plank's function in the interval of *Δλ*, we obtain:

$$\left(L_{\Delta\lambda}^{\downarrow Cirrus} - L_{\Delta\lambda}^{\downarrow Clear}\right)\left(z_o\right) = \bar{\varepsilon}_{\Delta\lambda} L_{\Delta\lambda}\left(T_{Cirrus}\right) \bar{\mathrm{t}}_{\Delta\lambda}\left(z_o, z_b\right) \tag{3-11}$$

Where $\bar{\mathrm{t}}_{\Delta\lambda}\left(z_o, z_b\right) = \dfrac{\int_{\Delta\lambda} t_{\lambda}\left(z_o, z_b\right) f(\lambda) d\lambda}{\int_{\Delta\lambda} f(\lambda) d\lambda}$.

Finally, the effective emissivity of the cirrus clouds in the interval *Δλ* is written by:

$$\bar{\varepsilon}_{\Delta\lambda} = \frac{\left(L_{\Delta\lambda}^{\downarrow Cirrus} - L_{\Delta\lambda}^{\downarrow Clear}\right)\left(z_o\right)}{\bar{\mathrm{t}}_{\Delta\lambda}\left(z_o, z_b\right) L_{\Delta\lambda}\left(T_{Cirrus}\right)} = \frac{\Delta L_{\Delta\lambda}^{\downarrow Cirrus}\left(z_o\right)}{\bar{\mathrm{t}}_{\Delta\lambda}\left(z_o, z_b\right) L_{\Delta\lambda}\left(T_{Cirrus}\right)} \tag{3-12}$$

The effective emissivity is obtained through a process of calculation by using the temperature profile from the Wyoming University sounding and the transmission from the radiative transfer code (Dubuisson et al, 2004).

4. Relation between the spectral emissivity and the size of the crystals in cirrus

A) Microphysical and optical parameters of cirrus

For modeling the radiative properties of cirrus, we must modeling the optical properties of ice crystals that makes up.

Their morphological and dimensional characteristics have a very high dispersion. The Figure (3-4) gives an idea of the multitude of shapes and sizes ranging from about 1 to 5,000 μm (Radke and Dowling, 1990). It depends for many of temperature (Heymsfield and Iaquinta, 2000). There are crystals of all shapes, in particular, recognizes the 'droxtals', the 'columns', the 'plates', the 'rosettes', or 'aggregates'.

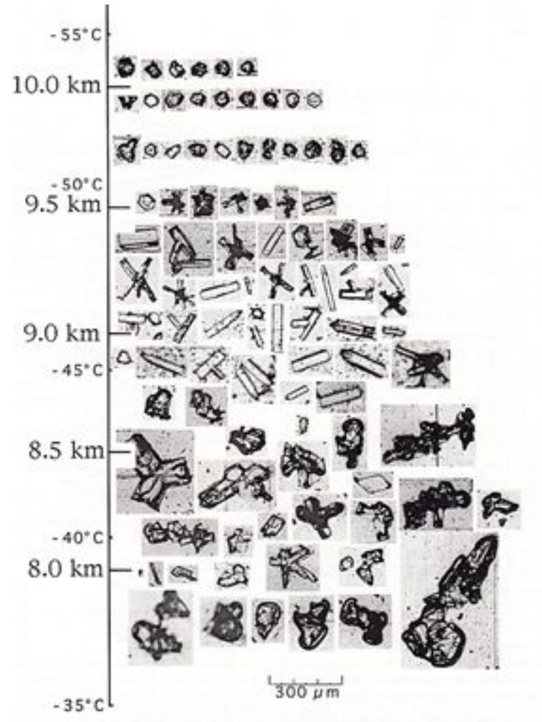

Figure (3-4)
Samples of ice crystals collected by an airborne campaign during the mission FIRE II.

Studies on the occurrence frequency of the different forms of ice crystals in cirrus clouds showed that the predominant forms are irregular shapes (Hallet and Korolev, 2000). Then, in this study, we first limit our study to an idealized type of crystals named 'aggregate' shown below:

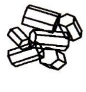

For the a given particle, optical properties are characterized by the efficiency factors of extinction, absorption and diffusion: Q_e , Q_a and Q_s. These dimensionless factors are connected by:

$$Q_e = Q_a + Q_s \tag{3-13}$$

and the single scattering albedo is defined by:

$$\varpi_o = \frac{Q_s}{Q_e} = \frac{Q_e - Q_a}{Q_e} \tag{3-14}$$

If G is the average projected area of the crystal, the effective extinction sections of absorption and scattering are written respectively: $C_e = Q_e G$, $C_a = Q_a G$ and $C_s = Q_s G$.

That will be a uniform distribution of crystals with identical crystals N per unit volume, we then define the extinction absorption and dissemination coefficients: $\sigma_e = NC_e$, $\sigma_a = NC_a$ and $\sigma_s = NC_s$.

At last, for a path length l in the medium, the optical thicknesses of extinction, absorption and diffusion are written:

$$\begin{cases} \delta_e = \sigma_e l \\ \delta_a = \sigma_a l \\ \delta_s = \sigma_s l \end{cases} \tag{3-15}$$

As shown in the Figure (3-5) and (3-6), the optical properties of such crystals, fairly representative samples, were calculated by Yang P., (2005).

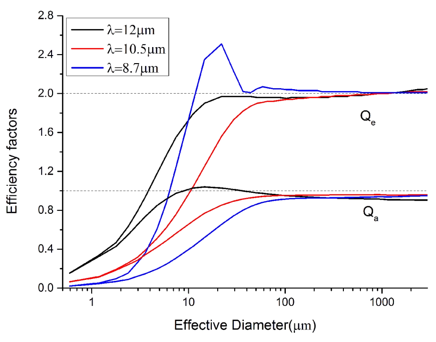

Figure(3-5)
Efficiency factors of the aggregate crystal by Yang P.

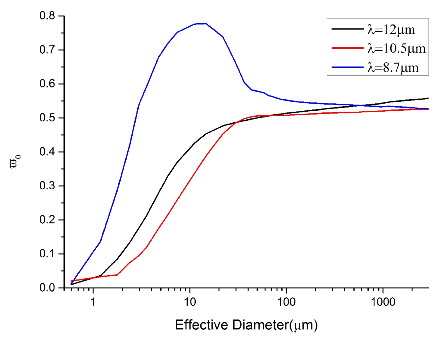

Figure (3-6)
Single scattering albedo of the aggregate crystal by Yang P.

For each of the spectral channel of the radiometer, we measure the variation of the efficiency factors and the single scattering albedo as function of the effective diameter of aggregates.

By identification with a sphere of radius R whose the volume is $\frac{4}{3}\pi R^3$ and the projected area is $S_p=\pi R^2$, we have the effective diameter is equal to $D=\frac{3V}{2S_p}$. For a crystal, this is the same definition of effective diameter.

B) Coefficient β as a function of the effective diameter

The hypothesis of the non scattering in cirrus cloud means that there is only absorption. For a path length l in the medium under consideration and two wavelengths λ_1 and λ_2, the transmissions are $t_1=\exp(-\delta_a^1)$ and $t_2=\exp(-\delta_a^2)$, where $\delta_a^1=\sigma_a^1 l$ and $\delta_a^2=\sigma_a^2 l$ are the are the absorption optical thicknesses. $\sigma_a^1$and σ_a^2 are the respective absorption coefficients for these two wavelengths:

$$\beta=\frac{\sigma_a(\lambda_1)}{\sigma_a(\lambda_2)}=\frac{Q_a(\lambda_1)}{Q_a(\lambda_2)}=\frac{1-\omega_0(\lambda_1)}{1-\omega_0(\lambda_2)}\frac{Q_e(\lambda_1)}{Q_e(\lambda_2)} \qquad (3\text{-}17)$$

From the Kirchhoff low and when the scattering effect is neglected, we obtain $\varepsilon=1-t$ and then we can write:

$$\varepsilon_2=1-(\varepsilon_1)^\beta \qquad (3\text{-}16)$$

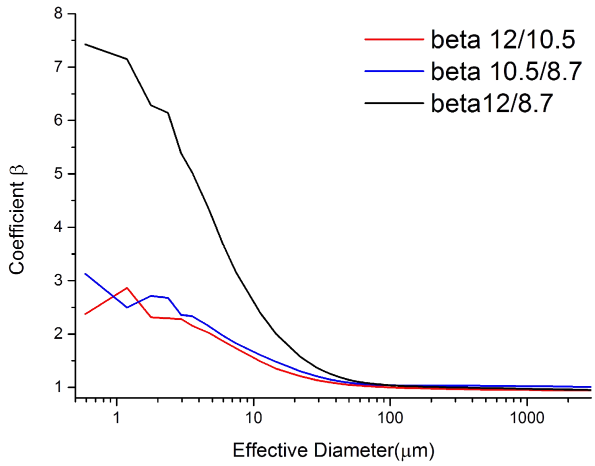

Figure (3-7)
Variation of the coefficient β for aggregate versus the effective diameter.

For the same crystal, we generally define the coefficient β which is the ratio of the two absorption coefficient corresponding to the wavelengths λ_1 and λ_2.

The Figure (3-7) presents the simulation results of the coefficient β. It turns out that the β12/8.7 parameter corresponding to the ratio is much more sensitive to the crystal size as those provided through other reports. To determine the effective diameter, I will use C12 and C09 to analysis.

5. Difference emissivity between C09 and C12

By using the difference of the emissivities, it's easy to distinguish the crystal diameter which is correspond to the coefficient β. In the Figure (3-8), we present the difference $\Delta\varepsilon=\varepsilon_2-\varepsilon_1=f(\varepsilon_1,\beta)$ with different values of the coefficient β ranging from 0.85 to 4.0. From equation (3-16), we can find easily:

$$\varepsilon_2-\varepsilon_1=\Delta\varepsilon=(1-\varepsilon_1)-(1-\varepsilon_1)^{\beta} \tag{3-18}$$

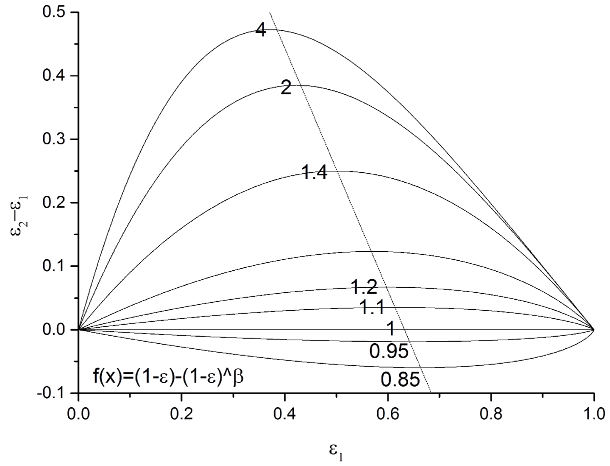

Figure (3-8)

The traces like 'arches' present the difference of the emissivity $\varepsilon_2-\varepsilon_1$ as function of ε_1; the straight line presents the locations of the maximums.

The differences are negligible for very thin cirrus ($\varepsilon_1\rightarrow0$) and for very thick cirrus ($\varepsilon_1\rightarrow1$ saturation effect).

A) The case where atmospheric transmission is not the same in both channels

We have considered instruments situated at M'Bour (Senegal) are located at about Z = 0 km above sea level. The vertical transmissions obtained from radiative transfer code and radiation sounding are shown in the table below. During the 3 months (January to March 2015), cirrus clouds are almost situated at around 10 km. The atmospheric transmission between 0 and 10 km of altitude is, in a first approximation, considered as constant (only the second decimal was affected). These transmissions are reported in Table (3-2).

Table (3-2) Transmission in of the atmosphere between Z=0 km and Z=10 km in M'Bour with two channels C09 and C12.

	C09	C12
$\bar{t}_{\Delta\lambda}(z_o, z_b)$	0.64	0.55

In this case, the transmission is not identical in the C09 and C12 channels, we write:

$$\varepsilon_1 = \frac{\varepsilon_1^*}{t_1}, \varepsilon_2 = \frac{\varepsilon_2^*}{t_2} \tag{3-19}$$

where $\mathrm{t}_1 = \bar{\mathrm{t}}_{C09}(z_o, z_b)$ and $\mathrm{t}_2 = \bar{\mathrm{t}}_{C12}(z_o, z_b)$

According to relation (3-19) and equation , we now have:

$$\Delta\varepsilon^* = \varepsilon_2^* - \varepsilon_1^* = (t_2 - \varepsilon_1^*) - t_2 t_1^{-\beta} (t_1 - \varepsilon_1^*)^{\beta} \tag{3-20}$$

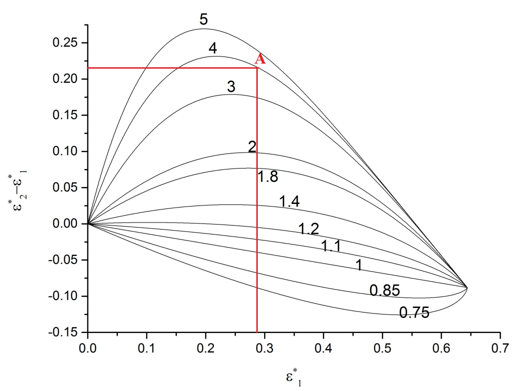

Figure (3-9)

The traces like arches present the difference of the emissivity $\varepsilon^*_2 - \varepsilon^*_1$ as function of ε^*_1; A is the data point corresponding to the measurements the $(\varepsilon^*_2 - \varepsilon^*_1, \varepsilon^*_1)$.

The variations of $\varepsilon^*_2-\varepsilon^*_1$ as function of ε^*_1 is presented in Figure (3-9) for different values of β between 0.75 and 5. Then, in the Figure (3-9), for each data point, it is possible to determine a coefficient β that allows to obtain a mean effective diameter of ice crystals in the studied cirrus.

6. Ice content of cirrus

Ice Water Path (IWP) of cirrus is an important parameter in the study of climate. Several authors have shown that there is a simple relationship between *IWP*, the infrared optical thickness and the effective diameter D_e crystals. Ebert and Curry (1992) established a relationship:

$$IWP \approx \delta \frac{D_e}{2.8} \tag{3-21}$$

where *IWP* is expressed in gm^{-2} and D_e in μm, δ is the cirrus optical thickness at λ=532 nm.

So the determination of optical thickness δ (by Lidar) and the effective diameter D_e can allow the determination of the ice content of cirrus.

Results

After using the method which is presented before, I get the results from the data of M'Bour (January to Match 2015). It contains the geometrical properties of the cirrus (altitude and the thickness), the optical properties (emissivity of TIR channels) and the effective diameter of the crystal.

1. Example of the studied cirrus

To explain the properties of the cirrus I have studied, I have given one example. In the Figure (4-1), we can see directly the altitude of the cirrus cloud. It is situated around 8 km during 3 hours in the vertical sky in 15th January 2015. The thickness of the cirrus in this period is around 300m. So this period can be considered as a perfect cirrus to study.

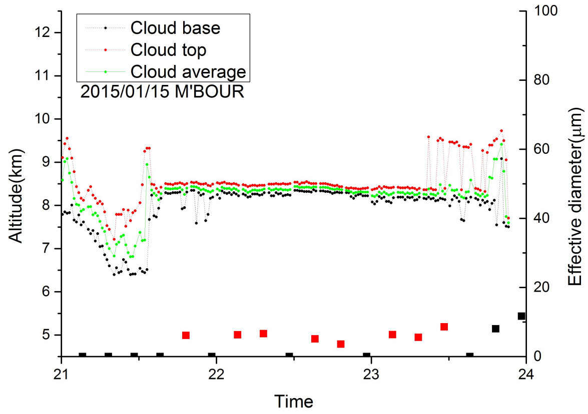

Figure (4-1)
The red point line presents the altitude of the cloud top; the green point line presents the average of the cloud; the black point line presents the altitude of the cirrus base.

In another expression, I have compared the result with the emissivity variation function. The Figure (4-2) shows that in this period, the coefficient β varies from 2 to 5.

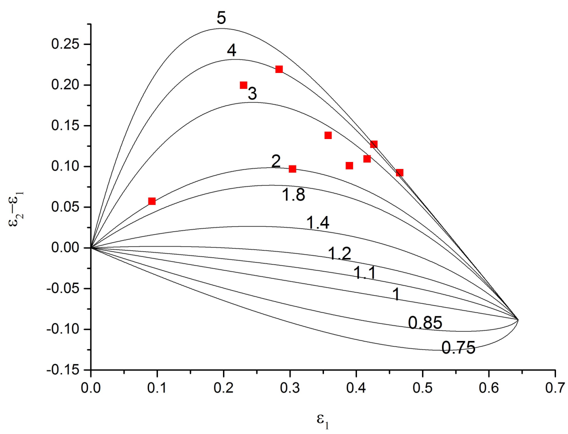

Figure(4-2)
The red squares present the measurement $\varepsilon_2-\varepsilon_1$ as function of ε_1 during the period we studied.

And then, for the same period, I presented the effective diameter of crystal in the Figure (4-3). We can see that the effective diameter is between 5 and 10 µm.

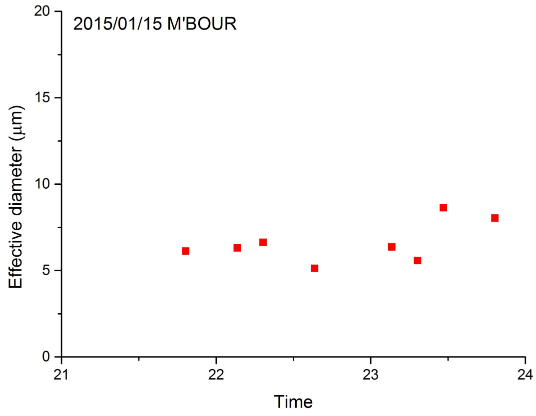

Figure (4-3)
The red squares present the effective diameter as a

2. Statistic results

M'Bour (Senegal) is situated in the west of the Africa continent. In the table (4-1), according to the cirrus cover time, in the first two months, cirrus cloud covered around 20% and situated at the altitude of around 9 km; in March, cirrus cloud covered around 8% and situated at the altitude of around 11 km. The IWP values which appears in the Table (4-1) is obtained from equation (3-21).

Table (4-1) Cirrus statistic characteristics between January and March 2015 in M'Bour (Senegal)

	January	February	March
Measure Time	429.7 h	601.3 h	596.7 h
Cirrus Time	95.6 h	114.5 h	50.3 h
Cirrus cover percentage	22.2%	19%	8.4%
Effective data point	574	687	302
Mean altitude [a]	8.47±0.13 km	9.14 ±1.87 km	11.46 ±3.19 km
Mean diameter [a]	49.2±15.8 µm	38.3 ±12.2 µm	40.1 ±11.4 µm
Ice Water Path [a]	10.3±1.6 gm^{-2}	9.6±1.7 gm^{-2}	8.7± 1.1 gm^{-2}

[a] Confidence interval with 95%

According to this statistic of altitude and effective diameter, in one hand, the cirrus cloud altitude increase during the 3 months, in another hand, the mean effective diameter of the crystal seems to decrease, not very strong effect in March. These results correspond to the measurement during the mission FIRE II, see Figure (3-4).

Conclusions

According to the results, this method works well. With this method, we can study the properties of cirrus cloud in a large extent. Tanks for the help of Mr. Brogniez and Mr. Parol, and other colleges. During this internship, I have learned deeply the theories about the radiative transfer, which helps me a lot to practice; I also was familiar with function of the Instrument Lidar and Thermal Infrared Radiometer, which helps me to understand the meaning of the measurement; The most important, I have searched the references about the cirrus cloud optical properties, which widens my knowledge about the cirrus research.

For the further research, there are some perspectives:

- Considering the scattering in the thermal infrared will help to get the precise effective emissivity, as well as taking into account the exact atmospheric transmission corresponding to each case.
- Considering the other different types of ice crystals in cirrus (columns, plates, droxtals, rosettes and so on) to study the different results obtained.
- Getting more data of the whole year will help to conclude the annual variation of the cirrus properties.
- The analysis of the data obtained at the different automatized stations in the world (Lille, Canary Islands, La Réunion) will help to obtain the seasonal and geographical cirrus characteristics.

Acknowledgments

I thank many people of the LOA for ensure that M'Bour automatically station works properly, especially Christine Deroo for the processing of the data and visualization on the LOA web site, Thierry Podvin, Luc Blarel and Philippe Goloub for the lidar data, Bahy Damiri and Yevgeny Derimian who check regularly the correct works of the TIR radiometer.

Bibliography

ANSMANN, Albert, BÖSENBERG, Jens, BROGNIEZ, Gérard. Lidar network observations of cirrus morphological and scattering properties during the International Cirrus Experiment 1989: the 18 October 1989 case study and statistical analysis. Journal of Applied Meteorology, 1993, 32, 10, 1608.

BROGNIEZ, G., BURIEZ, J. C., GIRAUD, V. Determination of effective emittance and a radiatively equivalent microphysical model of cirrus from ground-based and satellite observations during the International Cirrus Experiment: the 18 October 1989 case study. Monthly weather review, 1995, 123, 4, 1025.

BROGNIEZ, Gérard, PIETRAS, Christophe, LEGRAND, Michel. A high-accuracy multiwavelength radiometer for in situ measurements in the thermal infrared. Part II: Behavior in field experiments. Journal of Atmospheric and Oceanic Technology, 2003, 20, 7, 1023.

DOWLING, David R., RADKE, Lawrence F. A summary of the physical properties of cirrus clouds. Journal of Applied Meteorology, 1990, 29, 9, 970.

DUBUISSON, Philippe, GIRAUD, Vincent, PELON, Jacques. Sensitivity of thermal infrared radiation at the top of the atmosphere and the surface to ice cloud microphysics. Journal of Applied Meteorology and Climatology, 2008, 47, 10, 2545.

EBERT, Elizabeth E. CURRY, Judith A. A parameterization of ice cloud optical properties for climate models. Journal of Geophysical Research: Atmospheres (1984–2012), 1992, 97, D4, 3831.

FLAMANT, PIERRE, BROGNIEZ, G., DESBOIS, M.. High altitude cloud observations by ground-based lidar, infrared radiometer and Meteosat measurements. In: Annales geophysicae. Atmospheres, hydrospheres and space sciences, 1989, 1.

LYNCH, David K. Cirrus. Oxford University Press, 2001.

LEGRAND, Michel, PIETRAS, Christophe, BROGNIEZ, Gérard. A high-accuracy multiwavelength radiometer for in situ measurements in the thermal infrared. Part I: Characterization of the instrument. Journal of Atmospheric and Oceanic Technology, 2000, 17, 9, 1203.

LIOU, Kuo-Nan. Influence of cirrus clouds on weather and climate processes: A global perspective. Monthly Weather Review, 1986, 114, 6, 1167.

PAROL, F., BURIEZ, J. C., BROGNIEZ, G.. Information content of AVHRR channels 4 and 5 with respect to the effective radius of cirrus cloud particles. Journal of Applied Meteorology, 1991, 30, 7, 973.

RUSSELL, Philip B., SWISSLER, Thomas J., MCCORMICK, M.. Patrick. Methodology for error analysis and simulation of lidar aerosol measurements. Applied optics, 1979, vol. 18, no 22, p. 3783-3797.

YANG, Ping, WEI, Heli, HUANG, Hung-Lung. Scattering and absorption property database for nonspherical ice particles in the near-through far-infrared spectral region. Applied optics, 2005, vol. 44, no 26, p. 5512-5523.